Low GWP Refrigerants Modelling Study for a Room Air Conditioner Having Microchannel Heat Exchangers

Bo Shen[1]*, Mahabir Bhandari[1], Milind Rane[2], Deep Mota[2]

[1]Building Technologies Research and Integration Center, Oak Ridge National Laboratory
One Bethel Valley Road, P.O. Box 2008, MS-6070, Oak Ridge, TN 37831-6070
[2]Mechanical Engineering Department, Indian Institute of Technology Bombay, India
Email: shenb@ornl.gov, Telephone: 1-8655745745

ABSTRACT

Microchannel heat exchangers (MHX) have found great successes in residential and commercial air conditioning applications, being compact heat exchangers, to reduce refrigerant charge and material cost. This investigation aims to extend the application of MHXs in split, room air conditioners (RAC), per fundamental heat exchanger and system modelling. For this paper, microchannel condenser and evaporator models were developed, using a segment-to-segment modelling approach. The microchannel heat exchanger models were integrated to a system design model. The system model is able to predict the performance indices, such as cooling capacity, efficiency, sensible heat ratio, etc. Using the calibrated system and heat exchanger models, we evaluated numerous low GWP (global warming potential) refrigerants. The predicted system performance indices, e.g. cooling efficiency, compressor discharge temperature, and required compressor displacement volume etc., are compared. Suitable replacements for R22 and R-410A for the room air conditioner application are recommended.

1. INTRODUCTION

Micro-channel heat exchangers (MHX) use flat tubes with micro-channels, which reduce air side flow resistance and refrigerant charge. The micro-channels promote annular flow and thus effective refrigerant side heat transfer. Micro-channel heat exchangers have found great success in replacing condensers in commercial and residential air conditioners. However, MHXs are slow getting into the market of evaporators, because flat tubes impede water drainage, which negatively impacts defrosting and dehumidification performance, and distribution of two-phase flow to numerous mini-ports in a MHX evaporator is difficult. Technologies are actually available to overcome these barriers, for example, inserting a turbulator in the header entering the MHX to promote uniform mass flow distribution, coating the fins with water repellent layers, aligning the evaporator coil to facilitate water drainage, etc. These technical measures unavoidably cause extra cost, and make MHX evaporators less cost-effective than fin-tube evaporators.

The use of hydrofluorocarbon (HFC) refrigerants as non-ozone-depleting fluids alternatives for air-conditioning and refrigeration equipment was adopted by the developed countries during the ozone-depleting substances (ODS) phase-out as described in the Montreal Protocol. Unfortunately, most of the used HFCs have higher global warming potential (GWP) compared to the refrigerants that they replaced, which introduces uncertainty about their use in the future because of their impact on the climate, for example, R-410A has a GWP (AR4) of 2088, and R-22 has a GWP of 1810, which are thousands of times higher than natural refrigerants like CO2. HFCs currently account for only 1% of greenhouse gas emissions, but their use is growing rapidly, by as much as 10 to 15% per year, primarily because of their use as replacements for ODS and the increasing use of air conditioners globally, as reported by Ramanathan and Xu (2010 and 2013). Furthermore, according to the Montreal Protocol, Developing Countries, Article 5 Countries, have started their phase-down schedule for ODS. As such, finding suitable lower GWP refrigerants for HFC and hydrochlorofluorocarbon (HCFC) refrigerants is timely and will avoid a costly two-step transition from HCFC to HFC and then from HFC to lower-GWP refrigerants. Therefore, there is potential for significant reduction in greenhouse gas emissions through the substitution of high-GWP HFCs and HCFCs with lower-GWP alternatives. The low GWP refrigerant candidates are expected to reach a higher or similar efficiency level as compared to the refrigerants they will replace, to reduce in-direct global warming effect due to electricity consumption.

On the other hand, currently available low GWP refrigerants with good efficiencies for air conditioning applications all subject to flammability, for example, R-32 and propane. Their uses are prohibited in air conditioning systems, if the system charge exceeds a certain value. As mentioned, MHXs are effective in reducing system charge while maintaining similar heat transfer performance. They will extend the capacity range of flammable refrigerants without violating related safety regulations. Thus, conversion to flammable low GWP refrigerants makes it necessary to make air conditioners having all MHX heat exchangers, i.e. condenser and evaporator. This paper introduces development of MHX condenser and evaporator models, and integrating them to a system model.

2. Segment-to-Segment Microchannel Heat Exchanger Models

Segment-to-segment modeling approach can be used to model fin-tube (FTC) heat exchangers, by dividing each single tube into numerous segments. Microchannel heat exchangers can be modelled the same way, by each dividing single port into mini-segments. As shown in Figure 1, each port is divided to smaller segments. Heat transfer, pressure drop and charge inventory are calculated segment by segment. Each segmented control volume contains a single port. Heat transfer and pressure drop at the air and refrigerants sides are considered within each control volume. Air flows port-to-port along the micro-channel tube and fin surface.

There are many port shapes, for example, round, rectangular, trapezoidal, triangular, etc. The port hydraulic inside diameter is treated as the characteristic dimension to calculate heat transfer, pressure drop and void fraction. The real shape of a port is used to calculate its cross-sectional flow area for determining the inner volume, charge inventory, and inside heat transfer surface area. Each port's outside heat transfer surface area is calculated using the microchannel tube total outside surface area divided by its number of ports. The fins are treated as straight fins.

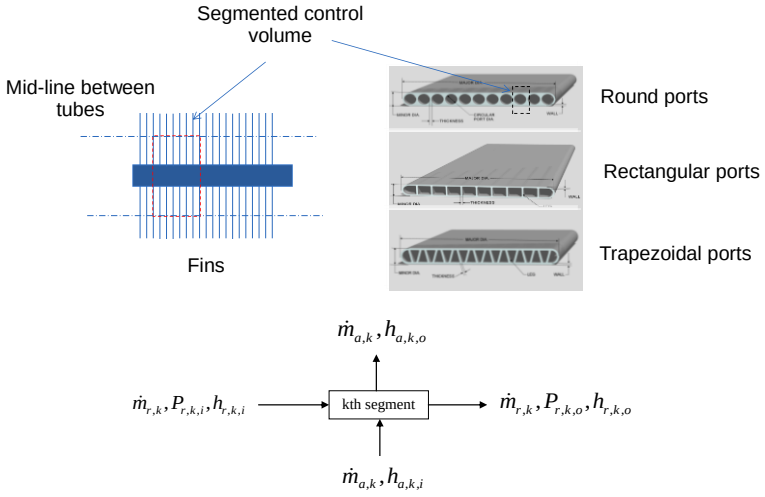

Figure 1: Segmented Control Volume of a Mini-Port

The heat transfer rate $\dot{Q}$ in each mini-segment is calculated using the $\varepsilon - NTU$ method. The pressure drop of the refrigerant $\Delta P_{r,k}$ is determined by the frictional pressure drop and momentum pressure drop within the port segment. In addition, the refrigerant mass in the tube segment can be determined with the known refrigerant properties and inner volume. The essence of using finite segments is that the substance properties can be treated as constant within each segment. Certainly, smaller segments lead to better accuracy. However, it is at the expense of calculation time.

Refrigerant-to-Air Heat Transfer:

For elements where no moisture condenses, the effectiveness correlations for sensible heat transfer are used to calculate the heat transfer between the refrigerant and air. The fin efficiency is calculated as Equation 1:

$$\eta_F = \frac{\tanh(mL_f)}{mL_f} \quad (1)$$

where η_F is the fin efficiency for heat transfer relative to the maximum heat transfer if the whole fin temperature is the same as the fin base temperature. L_f is the fin length in each control volume. In addition, $m = \sqrt{\frac{2h_o}{k_f \delta_f}}$, k_f is the fin thermal conductivity, h_o is the airside heat transfer coefficient, and δ_f is the fin thickness.

The overall efficiency relative to the entire surface area is calculated as,

$$\eta_o A_o = (A_o - A_F) + \eta_F A_F \tag{2}$$

where A_F is the fin surface area of each divided port, and A_o is the exposed port surface area including the port outside surface and the fin surface.

The overall heat transfer conductance UA is composed of three parts: the air side, the tube wall and the refrigerant side.

$$\frac{1}{UA} = R_o + R_{port} + R_i = \frac{1}{\eta_o A_o h_o} + R_{port} + \frac{1}{h_i A_i} \tag{3}$$

where h_i is the refrigerant side heat transfer coefficient, A_i is the port inside heat transfer area, and R_{port} is the tube wall thermal resistance, assuming each port is a mini round tube. A heat transfer correlation published by Dobson (1998) is used to calculate the condenser two-phase heat transfer coefficient. A pressure drop correlation published by Kedzierski (1999) is used to compute the two-phase pressure drop. The selected Air side heat transfer correlation was published by Kim and Bullard (2002).

Refrigerant-to-Air Heat & Mass Transfer

In the case of water condensing on an evaporating coil, both heat and mass transfer need to be considered. The effectiveness of heat and mass transfer is still defined as $\varepsilon^* = \frac{\dot{Q}}{\dot{Q}_{\max}}$. The approach for modeling a wet coil is based on Braun (1989). Braun (1989) introduced the parameter of the air saturation specific heat at the refrigerant temperature to model wet coils, where $c_s = (\frac{dh_{sat,air}}{dT})_{T=T_{ref}}$. Using the air saturation specific heat, the existing effectiveness relationships developed for sensible heat transfer can also be used for heat and mass transfer, based on the modified definitions for the number of transfer units and capacitance rate ratio. The details can be seen as follows:

The driving potential for heat transfer in the case of a wet coil is the difference between the enthalpies of the inlet air and the saturated air enthalpy at the refrigerant temperature. Then, the maximum possible heat transfer rate $\dot{Q}_{\max}$ is defined by:

$$\dot{Q}_{\max} = \dot{m}_a (h_{a,i} - h_{s,evap}) \tag{4}$$

Heat and mass transfer fin efficiency:

$$\eta_F^* = \frac{\tanh(m^* L_f)}{m^* L_f} \tag{5}$$

where $m^* = \sqrt{\frac{2h_o / C_{p,m}}{k_f / C_s \times \delta_f}}$, $C_{p,m}$ is the specific heat of the wet air. $\dot{m}_a$ is the air mass flow rate, $h_{a,i}$ is the air inlet enthalpy, $h_{s,evap}$ is the saturated air enthalpy at the refrigerant temperature. The overall heat and mass fin efficiency relative to the overall surface area is calculated as,

$$\eta_o^* A_o = (A_o - A_F) + \eta_F^* A_F \tag{6}$$

Overall heat and mass transfer conductance UA^*:

$$\frac{1}{U_o^* A} = \frac{C_{p,m}}{\eta_o^* h_o A_o} + C_s R_{tube} + \frac{C_s}{h_i A_i} \tag{7}$$

Modified number of transfer units NTU^* for the wet coil analysis:

$$NTU^* = \frac{U_o^* A_o}{\dot{m}_a} \tag{8}$$

Modified capacitance rate ratio for the wet coil analysis: $Cr^* = \frac{\dot{m}_a}{\dot{m}_r (C_{p,r} / C_s)}$ This parameter is used in a similar way in the heat and mass transfer analysis as C_r is used in the relationships for the effectiveness of the sensible heat transfer analysis. The flow-pattern-dependent heat transfer correlation published by Thome (2002) is used to calculate the evaporator two-phase transfer coefficient. The pressure drop correlation published by Kedzierski (1999) is used to model the two-phase pressure drop. The selected Air side heat transfer correlation was published by Kim and Bullard (2002).

Relationships of heat and mass transfer effectiveness ε^*: The heat and mass transfer effectiveness is a function of the modified number of transfer units and the modified capacitance rate ratio, $\varepsilon^* = f(NTU^*, Cr^*)$. The existing effectiveness models for sensible heat exchangers can then be used directly for wet coil analysis after using NTU^* to replace NTU, and Cr^* to replace C_r. The heat and mass transfer of a two-phase section is calculated by,

$$\varepsilon^* = 1 - \exp(-NTU^*) \tag{9}$$

For a single-phase section, the effectiveness correlations for cross-flow with one mixed (refrigerant) and one unmixed (air) fluid are used.

After the heat transfer rate $\dot{Q}$ is determined, the air side parameters can be obtained using the air side analysis. The air enthalpy flowing out of the segment is determined by,

$$h_{a,o} = h_{a,i} - \frac{\dot{Q}}{\dot{m}_a} \tag{10}$$

The saturation air enthalpy at the tube surface is

$$\bar{h}_{s,s,o} = h_{a,i} - \frac{h_{a,i} - h_{a,o}}{1 - \exp(-NTU_o^*)} \tag{11}$$

where $NTU_o^* = \frac{\eta_o^* h_o A_o}{\dot{m}_a c_{p,m}}$.

The effective tube surface temperature of the wet tube $\bar{T}_{s,o}$ is the saturated air temperature corresponding to the enthalpy of $\bar{h}_{s,s,o}$ at the barometric pressure.

Then the outlet air temperature can be determined using a sensible heat transfer calculation,

$$T_{a,o} = \bar{T}_{s,o} + (T_{a,i} - \bar{T}_{s,o}) \exp(-NTU_o) \quad (12)$$

where $NTU_o = \frac{\eta_o h_o A_o}{\dot{m}_{air} c_{p,m}}$ is for sensible heat transfer.

To model a port segment in an evaporator, the analysis can be conducted at first for the wet coil to decide the effective surface temperature $\bar{T}_{s,o}$. If $\bar{T}_{s,o}$ is smaller than the inlet dew point temperature, the coil is considered wet. Otherwise, the heat transfer rate is determined using the dry coil heat transfer analysis.

3. System Model

The micro-channel condenser and evaporator models were integrated to the DOE/ORNL Heat Pump Design Model (HPDM, Rice 1997 and Shen 2014) for system simulations. In the system model, basic efficiencies were adopted to model the compressor, i.e. volumetric efficiency shown in Equation 13, and isentropic efficiency shown in Equation 14.

$$m_r = Volume_{displacement} \times Speed_{rotation} \times Density_{suction} \times \eta_{vol} \quad (13)$$

$$Power = m_r \times (H_{discharge,s} - H_{suction}) / \eta_{isentropic} \quad (14)$$

Where m_r is compressor mass flow rate; $Power$ is compressor power; η_{vol} is compressor volumetric efficiency; $\eta_{isentropic}$ is compressor isentropic efficiency; $H_{suction}$ is compressor suction enthalpy; $H_{discharge,s}$ is an enthalpy obtained at the compressor discharge pressure and suction entropy.

To simulate low GWP refrigerants, interface functions were developed to call REFPROP 9.1 (Lemmon, 2010); and thus, HPDM accepts all the refrigerant types in the REFPROP 9.1 database, To speed up the property calculation, it has an option to generate property look-up tables, using REFPROP 9.1 and 1-D and 2-D cubic spline interpolation algorithms to calculate refrigerant properties, this would greatly boost the calculation speed, with the same accuracy.

Table 1 lists refrigerant types for this modeling study. In the table, R-32 is typically recommended as a low GWP refrigerant replacement of R-410A, and propane is recommended to replace R-22 in small size units. R-1234yf and R-1234ze are generally used as compositions of recent low GWP refrigerant mixtures, for example, DR-55 and DR-3.

Table 1: Selected Refrigerants

Refrigerant	GWP	Safety Class	Critical Temperature [°C]	Critical Pressure [kPa]
R-410A	1924	A1	71.3	4902
R-32	677	A2L	78.1	5782
R-22	1760	A1	96.2	4990
Propane	3	A3	96.7	4251
R-1234yf	4	A2L	94.7	3382
R-1234ze	6	A2L	109.4	3635

For the modeling study, we compare fin-tube evaporator and condenser to microchannel evaporator and condenser in one room air conditioner system having the same indoor and outdoor air flow rates. The FTC evaporator and condenser were obtained from a 1.5-ton (5.275 kW), split, ductless, room air conditioner, originally designed for R-22. The micro-channel condenser was from a similar capacity room air conditioner, originally design for R-410A.

The FTC heat exchangers and MHX condenser were modeled and calibrated against experimental data, by adjusting the air side heat transfer multipliers. The MHX evaporator is modelled to replace the FTC evaporator in Table 2, having the same frontal flow area. The MHX evaporator uses the same type of micro-channel tubes as the MHX condenser. The MHX evaporator is assumed to have ideal refrigerant mass flow distribution and drainage of condensed water, and adopts the air side heat transfer multiplier of the MHX condenser model. Inlet and outlet headers of the MHXs have an outside diameter of 1 inch (25.4 mm). Because the one-row MHX condenser has smaller fin surface area of individual fins, it needs larger fin density than the two-row fin-tube condenser, i.e. 1.125 times as dense, to accomplish the same heat duty. Similarly, it is assumed that the one-row MHX evaporator has 1.125 times of fin density as the two-row fin-tube evaporator. For the MHXs, the flat tubes reduce air flow resistance; however, the increased fin densities increase the flow resistance. There is a trade-off, and the fan powers consumed by the MHXs are similar to fin-tube heat exchangers. For this modeling study, we only evaluated one-row evaporator, as adding another row will result in no charge reduction in the evaporator.

Table 2: Heat Exchanger Dimensions

Outdoor Heat Exchanger (Condenser)		
Type	Fin-tube coil	Microchannel
Total Tube Number	52	65
Number of rows	2	1
Number of parallel circuits	(3 condensing +1 subcooling)	(47 cond + 18 in subc)
Fin density (fins/m)	629.9	708.7
Frontal flow area [m^2]	0.587	0.550
Tube diameter [mm]	8.15 (outside diameter)	0.8 (hydraulic d_i)/14 ports
Tube Length [m]	0.89	0.89
Air Flow [m^3/s]/Fan Power [W]	1.369 m^3/s /196 W	
Indoor Heat Exchanger (Evaporator)		
Type	Fin-tube coil	Microchannel
Total Tube Number	32	42
Number of rows	2	1
Number of parallel circuits	4	42
Fin density (fins/m)	787.4	885.9
Frontal flow area [m^2]	0.285	0.285
Tube diameter [mm]	7.2 (outside diameter)	0.8 (hydraulic d_i)/14 ports
Tube Length [m]	0.813	0.813
Air Flow [m^3/s]/Fan Power [W]	0.243 m^3/s /52.5 W	

4. Simulation Results

In the system modelling, the compressor volumetric efficiency was set at 90% and the isentropic efficiency was set at 70%. The compressor shell heat loss was assumed to be 5% relative to the compressor power. The condenser exit subcooling degree was specified at 10R (5.6K), and the evaporator exit superheat degree was also set at 10R (5.6K). Simulations were performed for all the selected refrigerants at the AHRI 210/240 standard A rated condition, i.e. ambient air temperature at 95°F (35°C) and indoor air at 80°F (26.6°C) dry bulb/67°F (19.4°C) wet bulb. The compressor displacement was auto-calculated to match a target cooling capacity of 1.5-ton (5.275 kW).

Figure 2 illustrates predicted charges summed in the condenser and evaporator, for the system using MHXs and FTCs, respectively. It can be seen that the MHXs reduce the charge up to 55%, consistently for all the refrigerants. Although propane is the most flammable refrigerant, it has the least charge, i.e. less than 0.5 lbs (0.23 kg). Consequently, it is feasible to use propane in small capacity room air conditioners, having all micro-channel heat exchangers. It should be mentioned that Hughmark (1956) was used to calculate the void fractions in both MHX and FTC heat exchanger models.

Figures 3 and 4 shows predicted compressor suction and discharge saturation temperatures, which indicate overall heat transfer performance in the evaporator and condenser. There are two major factors impacting the overall heat transfer performance, one is the air side and refrigerant side heat transfer coefficient and surface area, the other is the

refrigerant saturation temperature drop. The saturation temperature drop, as illustrated in Figures 5 and 6, incurs with the refrigerant pressure drop. Large temperature drop decreases the average temperature driving difference between the air side and refrigerant side, which pushes suction pressure lower or discharge pressure higher for achieving the same heat duty. Figure 3 indicates that the FTC evaporator has better heat transfer performance than the MHX evaporator, for R-410A, R-32, R-22 and propane because it has larger heat transfer surface area. However, the FTC evaporator appears worse for R-1234yf and R-1234ze, because these two refrigerants' saturation temperature drops are very sensitive to the pressure drop in the evaporator, and the MHX evaporator is able to decrease the pressure drop when having multiple, parallel flat tubes and mini ports. At the condenser side, the MHX results in slightly better heat transfer performance i.e. lower discharge saturation temperatures for all the refrigerants, due to the smaller saturation temperature drops.

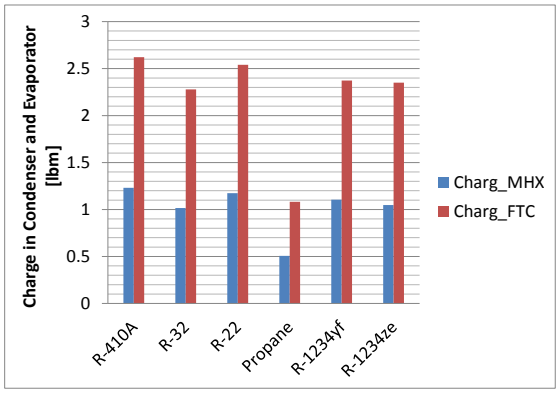

Figure 2: Summed charge in condenser and evaporator

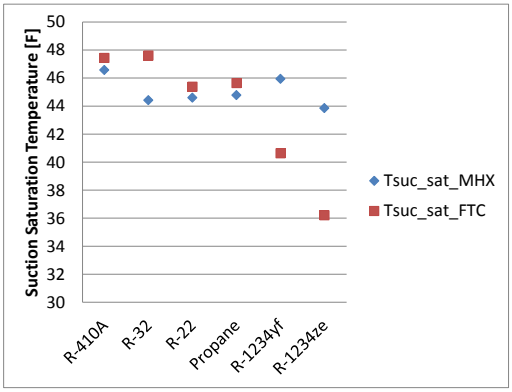

Figure 3: Suction saturation temperatures

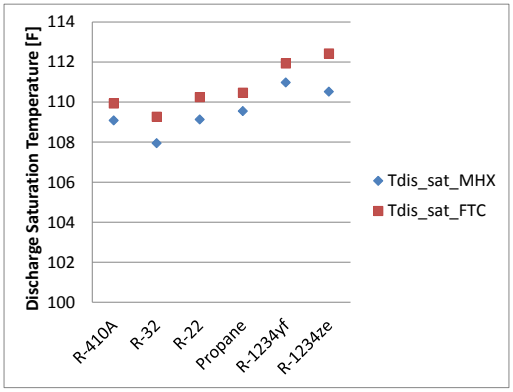

Figure 4: Discharge saturation temperatures

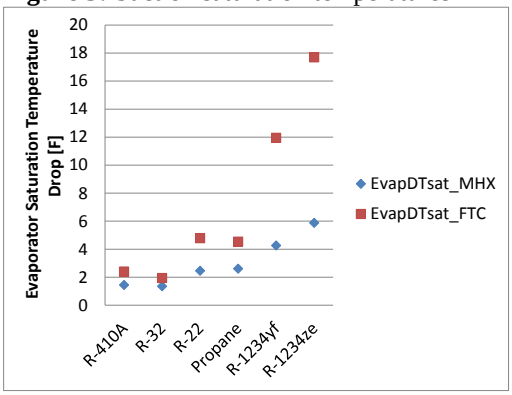

Figure 5: Evaporator saturation temperature drops

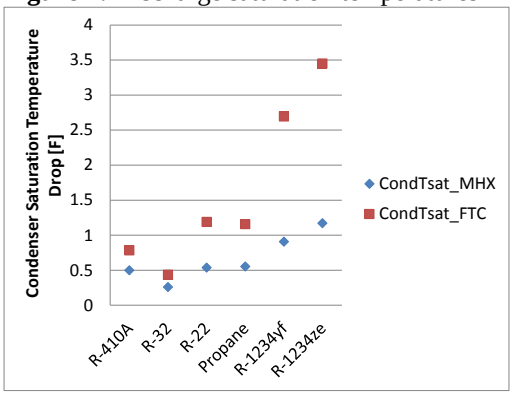

Figure 6: Condenser saturation temperature drops

Figure 7 shows predicted sensible heat ratios with using MHX and FTC, which presents no apparent difference among the refrigerants. On the other hand, the MHX evaporator has 2% higher SHR, indicating it is less effective in water removal, due to its shorter air flow path. Figure 8 illustrates predicted compressor discharge temperatures. R-32 appears to have the highest discharge temperature. Propane, R-1234yr and R-1234ze have lower discharge temperatures. Figure 9 presents the required compressor displacement volumes, as ratios to the volume of R-410A system using FTCs. It can be seen that R-32 and R-410A require a similar displacement volume to achieve the cooling capacity of 1.5-ton (5.275 kW). R-1234yf and R-1234ze require much larger displacement volumes, i.e. 2 to 3 times as large, implying those refrigerants will use more expensive compressor products later. Figure 10 shows predicted COPs. Due to the heat transfer performance differences observed in Figures 3 to 6, the MHXs lead to significantly better COPs for R-1234yf and R-1234ze than FTCs, due to reducing the saturation temperature drops, but worse COPs for the other refrigerants due to the smaller surface area. In general, R-32 has the highest COP. R-22 and propane have comparable COPs. R-1234yf and R-1234ze have the lowest COPs. If the MHXs are used, their COPs can be increased to 95% COP of R-32.

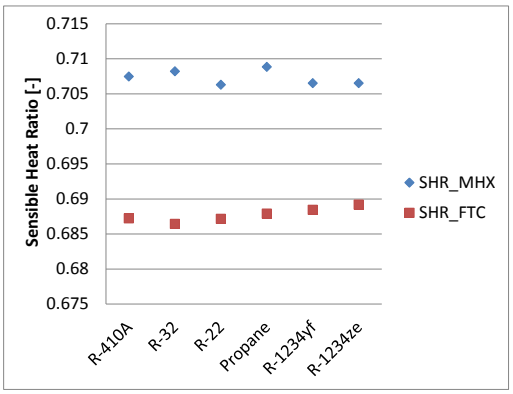

Figure 7: Sensible heat ratios

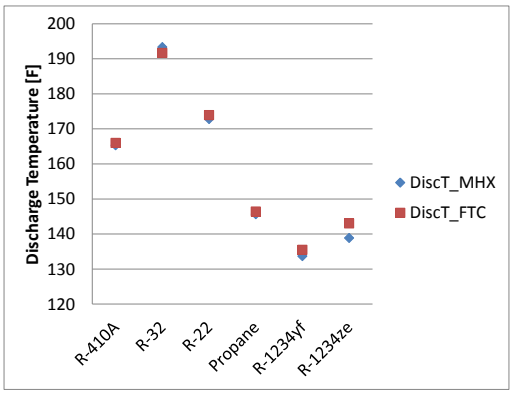

Figure 8: Compressor discharge temperatures

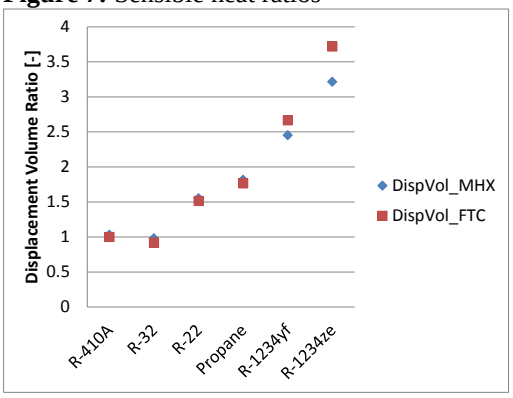

Figure 9: Compressor displacement volumes

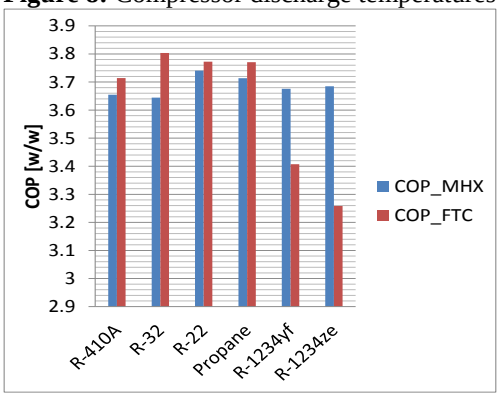

Figure 10: Cooling COPs

3. Summary

This paper introduces modelling microchannel condenser and evaporator by dividing each single port into numerous segments (segment-to-segment modelling approach). The MHX models were integrated to a system model. The system model was used to assess performances of R-410A, R-32, R-22, Propane, R-1234yf and R-1234ze in a 1.5-ton (5.275 kW) room air conditioner, using FTC or MHX heat exchangers, respectively. The system modelling results demonstrate that the MHXs effectively reduce the system charge, and can be useful to extend the application range of a flammable refrigerant, like propane. The one-row MHX evaporator enhances the system performances of R-1234yf and R-1234ze, because it reduces the heat exchanger saturation temperature drop, and benefits the overall heat transfer performance. On the other hand, the MHX evaporator leads to worse system performances for R-410A, R-32, R-22 and propane, due to its limited tube and fin surface area.

R-32 has the best system performance and requires a similar compressor displacement volume as R-410A. R-1234yf and R-1234ze have the worst performances and require much larger compressor displacement volumes. Nonetheless, use of MHXs is most effective in enhancing the system performances of R-1234yf and R-1234ze. R-22 and propane have a similar performance, but propane requires a larger compressor displacement volume.

REFERENCES

Braun. J.E., Klein. S.A, and Mitchell, J.W., 1989, "Effectiveness models for cooling towers and cooling coils", ASHRAE Transactions, 95(2), pp. 164-174.

Dobson M. K. and Chato J. C., 1998 "Condensation in Smooth Horizontal Tubes", Journal. Heat Transfer 120(1), 193-213 (Feb 01, 1998)

Hughmark, G. A., 1962, "holdup in gas-liquid flow," Chem. Eng. Progress, Vol. 58, PP. 62-65

Kedzierski, M. A., and Choi J. Y., "A generalized pressure drop correlations for evaporation and condensation of alternative refrigerants in smooth and micro-fin tubes" NISTIR 6333, 1999

Kim Man-Hoe, Bullard Clark W., 2002, "Air-side thermal hydraulic performance of multi-louvered fin aluminum heat exchangers.", International Journal of Refrigerant, No. 25, pp 390-400.

Lemmon Eric W., Huber Marcia L. (2010) "NIST Reference Fluid Thermodynamic and Transport Properties Database (REFPROP): Version 9.1", http://www.nist.gov/srd/upload/REFPROP9.PDF

Rice, C. K., 1997. "DOE/ORNL Heat Pump Design Model, Overview and Application to R-22 Alternatives",3rd International Conference on Heat Pumps in Cold Climates, Wolfville, Nova Scotia, Canada, Aug. 11-12, 1997; Caneta Research, Inc., Mississauga, Ontario, Canada, November, pp.43-66.

Ramanathan and Y. Xu (2010). "The Copenhagen Accord for Limiting Global Warming: Criteria, Constraints, and Available Avenues," Proc. Natl. Acad. Sci. USA 107, 8055–8062.

Shen, B. and Rice, C. K., 2014, HVAC System Optimization with a Component Based System Model – New Version of ORNL Heat Pump Design Model, Purdue HVAC/R Optimization short course, International Compressor & refrigeration conferences at Purdue, Lafayette, USA, 2014; web link: http://hpdmflex.ornl.gov/hpdm/wizard/welcome.php

Thome J.R. and Jean Ei Hajal, 2002, "On recent advances in modelling of two-phase flow and heat transfer", 1st Int. Con. on Heat Transfer, Fluid mechanics, and Thermodynamics, Kruger Park, south Africa TJ1, 8-10 April.

Thome J. R., J. El Hajal, and A. Cavallini, 2003a, "Condensation in horizontal tubes, part 1: two-phase flow pattern map", International Journal of Heat and Mass Transfer, 46(18), Pages 3349-3363.

Thome J. R., J. El Hajal and A. Cavallini, 2003b, "Condensation in horizontal tubes, part 2: new heat transfer model based on flow regimes", International Journal of Heat and Mass Transfer, 46(18), Pages 3365-3387.

ACKNOWLEDGEMENT

The authors thank Mr. Antonio Bouza, Technology Development Manager for HVAC, WH, and Appliances, Emerging Technologies Program, Buildings Technology Office at the U.S. Department of Energy for supporting this research project.